Supporting Information

Ion Pair Organic Frameworks Based on Multitopic Ultracycles for Efficient Iodine Absorption

Teng-Yu Huang,† Wen-Hui Mi,† Xu-Dong Wang, Yu-Fei Ao, De-Xian Wang* and Qi-Qiang Wang*

E-mail: dxwang@iccas.ac.cn, qiqiangw@iccas.ac.cn

Contents

1. General Information

All Chemicals were obtained from commercial sources and used without further purification unless stated otherwise. NMR spectra were recorded on Bruker 400 and 500 MHz NMR spectrometers at room temperature. Chemical shifts are reported in ppm and referenced to tetramethylsilane or the residual solvent signal. Mass spectra were measured on a Nicolet-6700 FI-IR spectrometer with KBr pellets in the 400−4000 cm^{-1} region. Elemental analysis was recorded on Carlo Erba 1106. Melting points are uncorrected. X-ray diffraction was performed on Rigaku R-AXIS RAPID IP.

2. Synthesis and Characterization

2.1 Synthesis and characterization of macrocyclic precursors

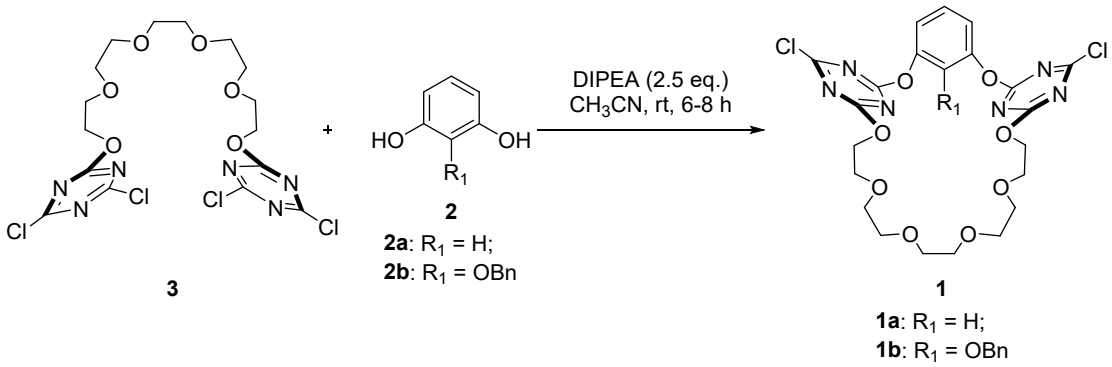

Scheme S1. Synthesis of macrocyclic precursors.

Synthesis of **1a**[S1]. **3**[S2] (2.40 g, 4.92 mmol) and resorcinol **2a** (0.54 g, 4.92 mmol) were dissolved in 500 mL of acetonitrile. To this solution was added DIPEA (1.53 g, 11.80 mmol) dropwise in 100 mL acetonitrile during a period of 2 h, and then kept stirring for 6 h, and then the solvent was removed under vacuum by a rotary evaporator. The residue was chromatographed on silica gel (100–200 mesh) with a mixture of ethyl acetate and petroleum ether (1:1, v/v) as the eluent to yield **1a** (1.20 g, 43%) as white solid.

1a:^{1}H NMR (500 MHz, $CDCl_3$) δ (ppm) 7.49 (t, J = 8.3 Hz, 1H), 7.19 (t, J = 2.2 Hz, 1H), 7.13 (dd, J = 8.3 Hz, 2.2 Hz, 2H), 4.51 (t, J = 4.5 Hz, 4H), 3.78 (t, J = 4.6 Hz, 4H), 3.61–3.58 (m, 8H), 3.57 (s, 4H); ^{13}C NMR (125 MHz, CD_3CN): δ (ppm) 173.8, 173.4, 173.1, 153.1, 131.7, 120.6, 116.6, 71.3, 71.27, 71.25, 69.6, 69.2.

Synthesis of **1b**. **3** (1.07 g, 2.00 mmol) and OH derivative substituted diphenol **2b**[S3] (0.44 g, 2.00 mmol) were dissolved in 200 mL acetonitrile. To this solution was added DIPEA (0.65 g, 5.00 mmol) dropwise in 60 mL acetonitrile during a period of 0.5 h, and then kept stirring for 5.5 h, and then the solvent was removed under vacuum by a rotary evaporator. The residue was chromatographed on silica gel (100–200 mesh) with a mixture of ethyl acetate and petroleum ether (1:1, v/v) as eluent, yielding 1b (0.63 g, 46%) as white solid.

1b: mp 38−41 °C; ^{1}H NMR (DMSO-d_6, 500 MHz) δ (ppm) 7.37–7.21 (m, 6H), 7.12 (s, 2H), 4.92 (s, 2H), 4.38 (t, J = 4.4 Hz, 4H), 3.67 (t, J = 4.6 Hz, 4H), 3.46 (m, 12H); ^{13}C NMR (DMSO-d_6, 125 MHz) δ (ppm) 172.4, 172.2, 171.8, 145.2, 142.4, 136.6, 128.6, 128.5, 127.8, 124.5, 121.6, 75.5, 70.3, 68.9, 68.2; IR (KBr) ν 3201, 3059, 2877, 2803, 1700, 1455, 1397, 1094, 1060, 545 cm^{-1}; HR-ESI-MS (positive ion mode) m/z: $[M+H]^+$ calcd for $C_{29}H_{31}Cl_2N_6O_9$: 677.1524, found: 677.1518; Anal. Calcd (%) for $C_{29}H_{30}Cl_2N_6O_9 + H_2O$: C, 48.82; H, 4.80; N, 11.78, found: C, 48.89; H, 4.96; N, 11.73.

2.2 Synthesis and characterization of ultracycles

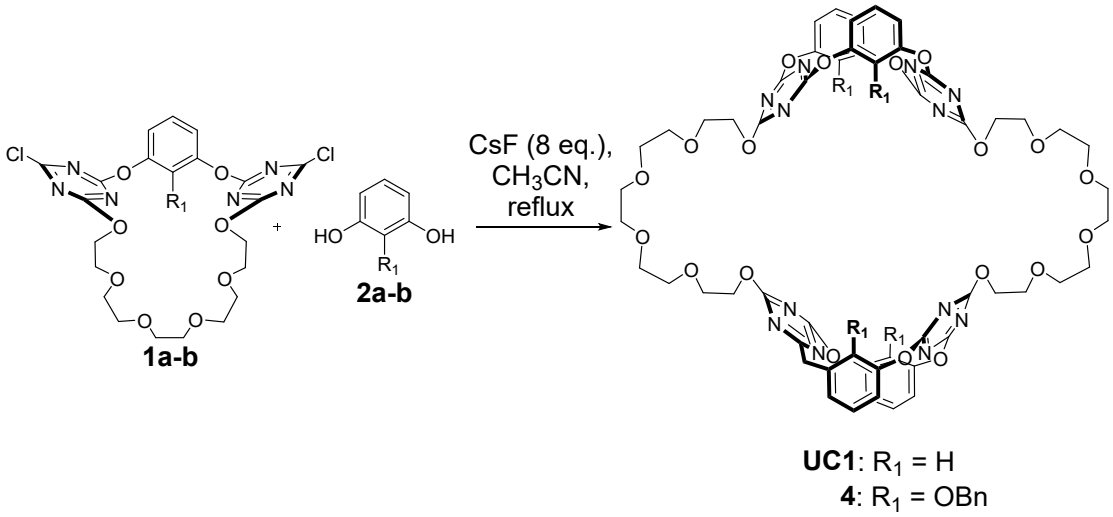

Scheme S2. Synthesis of ultracycle **UC1** and precursor **4**.

Synthesis of **UC1**. **1a** (2.86 g, 5.00 mmol), resorcinol **2a** (0.55 g, 5.00 mmol), and cesium fluoride (6.05 g, 40.00 mmol) were added into 500 mL dry acetonitrile. Then, the mixture was allowed to reflux for 2 h under an argon atmosphere. After cooled to room temperature, the mixture was filtered, the filtrate was concentrated in vacuum by a rotary evaporator, and then chromatographed on silica gel (100–200 mesh) with mixture of dichloromethane and acetone (5:1–3:1, v/v) as eluent to yield **UC1** (552 mg, 18.2%) as white solids.

UC1: ^{1}H NMR ($CDCl_3$, 500 MHz) δ (ppm) 7.20 (t, J = 8.2 Hz, 4H), 6.82 (dd, J = 8.2, 2.0 Hz, 8H), 6.67 (t, J = 2.0 Hz, 4H), 4.66 (t, J = 4.5 Hz, 8H), 3.91 (t, J = 4.5 Hz, 8H),

3.75–3.69 (m, 24H); ^{13}C NMR ($CDCl_3$, 125 MHz,): δ (ppm) 174.2, 173.3, 152.0, 130.1, 119.2, 116.7, 70.9, 70.8, 68.9, 68.2.

Synthesis of **4**. **1b** (1.88 g, 3.00 mmol), **2b** (0.65 g, 3.00 mmol) and cesium fluoride (3.65 g, 24.00 mmol) were added into 300 mL dry acetonitrile. Then, the mixture was allowed to reflux for 1.5 h under argon atmosphere. After cooled to room temperature, the mixture was filtrated, and the filtrate was concentrated under vacuum by a rotary evaporator and then chromatographed on silica gel (100–200 mesh) with mixture of dichloromethane and acetone (6:1–4:1) as eluent to yield **4** (155 mg, 6.3%) as white solids.

4: mp 51−53 °C; ^{1}H NMR (d_6-DMSO, 500 MHz) δ (ppm) 7.07–6.99 (m, 24H), 6.91 (d, J = 7.2 Hz, 8H), 4.72 (s, 8H), 4.39 (t, J = 4.5 Hz, 8H), 3.70 (t, J = 4.5 Hz, 8H), 3.57–3.53 (m, 24H); ^{13}C NMR (DMSO-d_6, 125 MHz) δ (ppm) 174.0, 173.1, 145.3, 142.7, 136.6, 128.3, 128.0, 127.2, 124.2, 121.1, 74.9, 70.4, 70.3, 70.3, 68.4, 68.2; IR (KBr) ν 2876, 1577, 1557, 1486, 1382, 1335, 1281, 1238, 1119, 814, 750 cm^{-1}; HR-ESI-MS (positive ion mode) m/z: $[M+Na]^+$ calcd for $C_{84}H_{80}N_{12}O_{24}Na$: 1663.5301, found: 1663.5314; Anal. Calcd (%) for $C_{84}H_{80}N_{12}O_{24}$: C, 61.46; H, 4.91; N, 10.24, found: C, 61.19; H, 4.90; N, 10.09.

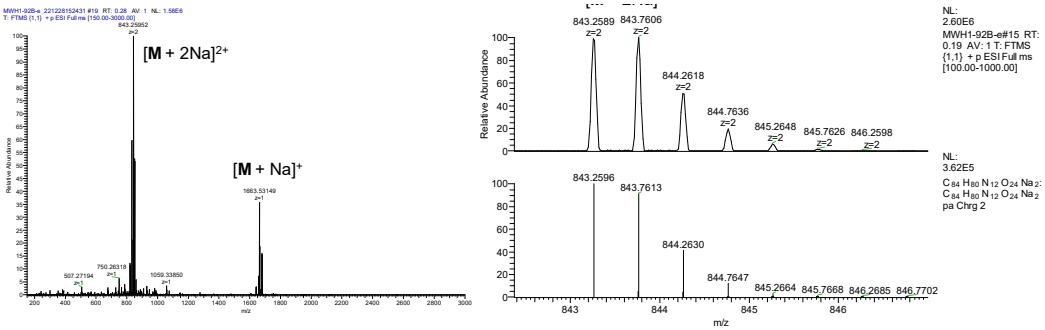

Figure S1. HR-ESI-MS of spectra of **4**.

2.3 Debenzylation of ultracycles 4.

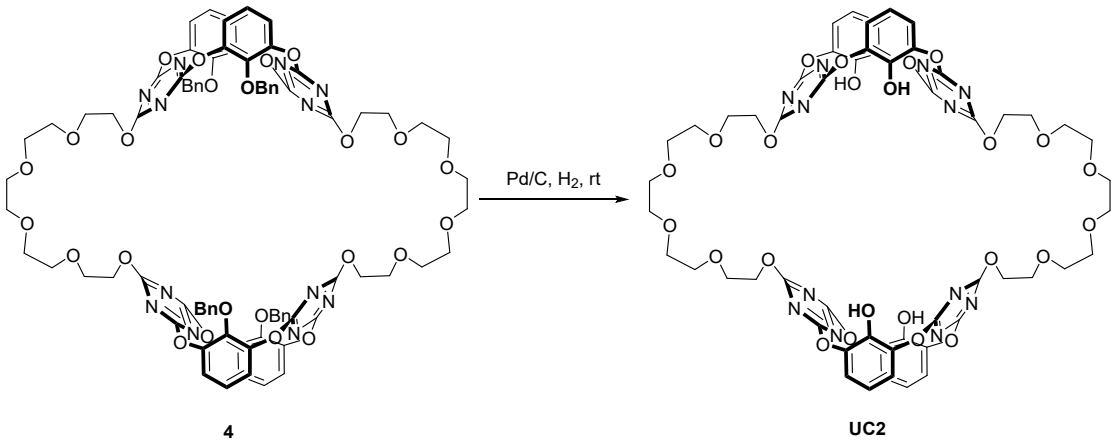

Scheme S3. Debenzylation of ultracycles **4**.

Synthesis of **UC2**. At room temperature, **4** (100 mg, 0.0609 mmol), Pd/C (40 mg) and THF (20 mL) were mixed in a two-neck flask. The mixture was stirred for 24 h under H_2 balloon. After filtration with diatomaceous earth, the filtrate was concentrated under vacuum by a rotary evaporator. The residue was recrystallized with methanol, dichloromethane, acetonitrile and ethyl ether to give purified compound **UC2** (45 mg, 58%) as white solid.

UC2: mp 42−44 °C; ^{1}H NMR (DMSO-d_6, 500 MHz) δ (ppm) 9.38 (s, 4H), 6.85 (d, J = 8.0 Hz, 8H), 6.63 (t, J = 8.4 Hz, 4H), 4.59 (t, J = 4.7 Hz, 8H), 3.83–3.76 (t, J = 4.0 Hz, 8H), 3.62–3.60 (m, 8H), 3.57–3.55 (m, 16H); ^{13}C NMR (DMSO-d_6, 125 MHz) δ (ppm) 173.9, 173.2, 142.2, 141.1, 120.4, 118.6, 70.3, 70.3, 70.3, 68.65, 67.9; IR (KBr) v 2876, 1577, 1500, 1394, 1335, 1259, 1119, 815 cm^{-1}; HR-ESI-MS (negative ion mode) m/z: [M−H]$^-$ calcd for $C_{56}H_{55}N_{12}O_{24}$: 1279.3447, found: 1279.3468; Anal. Calcd (%) for $C_{56}H_{56}N_{12}O_{24}$: C, 52.50; H, 4.41; N, 13.12, found: C, 52.05; H, 4.44; N, 12.73.

3. Ion-pair Screening

With the multitopic ultracycles in hand, we took **UC1** and **UC2** ultracycles to investigate their ion pair binding ability using ^{1}H NMR spectra. The experiments were performed by dissolving the ultracycles in $CDCl_3$, and solid alkali and alkaline earth salts were added to the solution to allow solid-liquid extraction if ion binding is possible. Spectra of the ultracycles with and without the presence of salts were then monitored and compared. Due to the poor solubility of the applied salts in $CDCl_3$, simultaneous chemical shift changes of aromatic or hydroxyl protons (anion binding site) and glycol chains (cation binding site) could reflect the ion pair binding behavior (solid–liquid extraction). We categorized our observations into the following four ion pair binding types:

1) inactive chemical shifts suggest no detectable ion pair interactions (denoted as "***N***" in the **Table S1**, **Figure S2**);

2) chemical shift changes in a fast exchange process relative to the NMR time scale indicate ion pair interactions (denoted as "***F***" in the **Table S1**, **Figure S3**);

3) significant chemical shift changes in a slow exchange process reflect strong ion pair interactions (denoted as "***S***" in the **Table S1**, **Figure S4**);

4) disappearance of the NMR signals as a result of host-guest co-precipitation (denoted as "P" in **Table S1**, **Figure S5**).

Table S1. Results for solid–liquid extraction of **UC1** and **UC2**

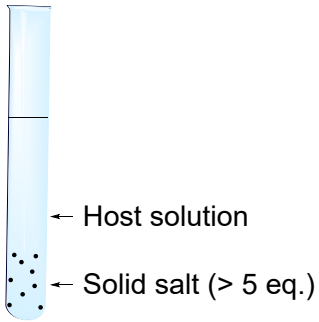

Ion-pair	Results for solid–liquid extraction	
	UC1	**UC2**
LiCl	***N***	***N***
LiBr	***F***	***F***
LiI	***F***	***F***
NaCl	***N***	***F***
NaBr	***N***	***F***
NaI	***F***	***F***
KCl	***N***	***F***
KBr	***N***	***F***
KI	***N***	***F***
$CaCl_2$	***N***	***F***
$CaBr_2$	***S***	***P***
CaI_2	***P***	***F***
$SrCl_2$	***N***	***F***
$SrBr_2$	***N***	***F***
SrI_2	***P***	***F***

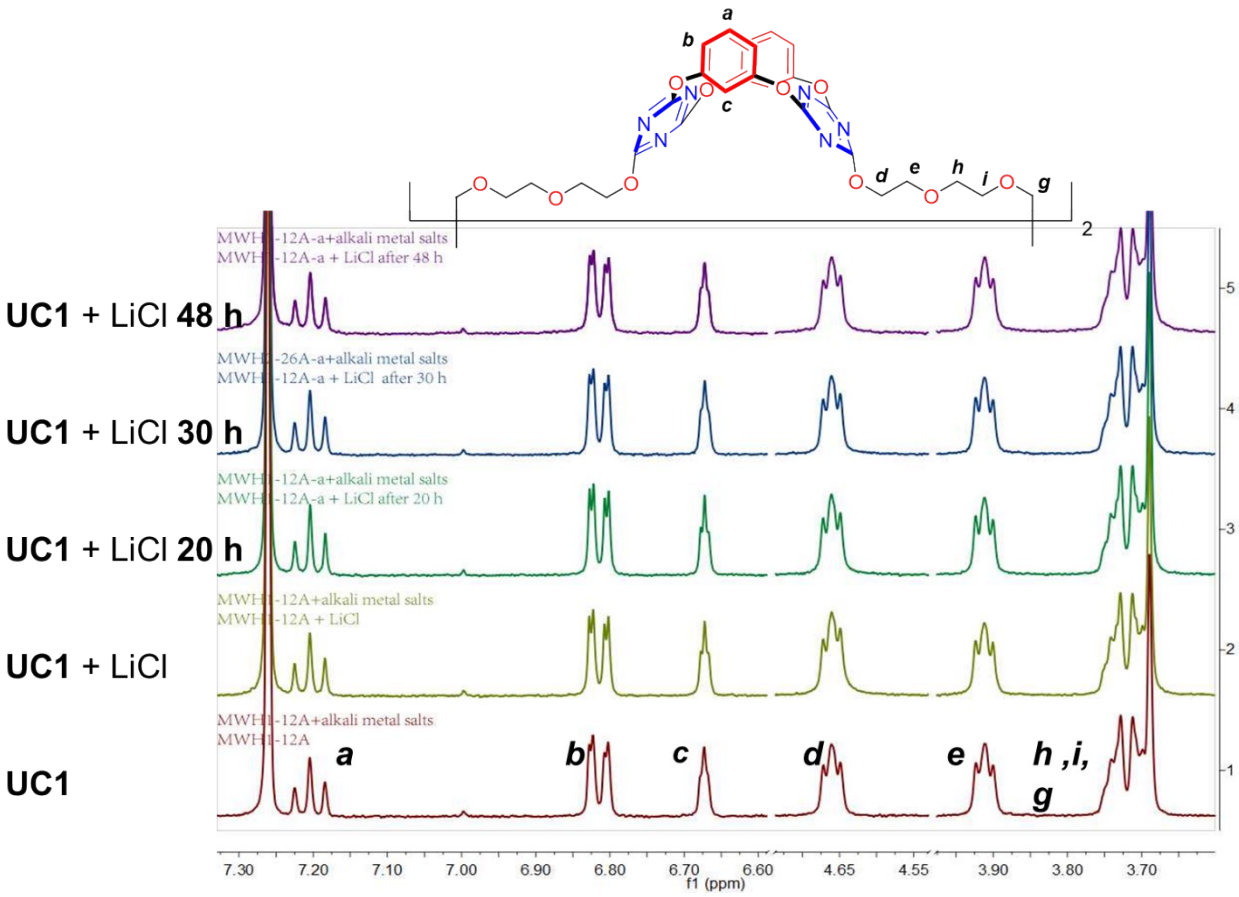

Figure S2. ^{1}H NMR spectra of solid-liquid extraction of **UC1** (10^{-3} M) and LiCl at different times ("***N***")

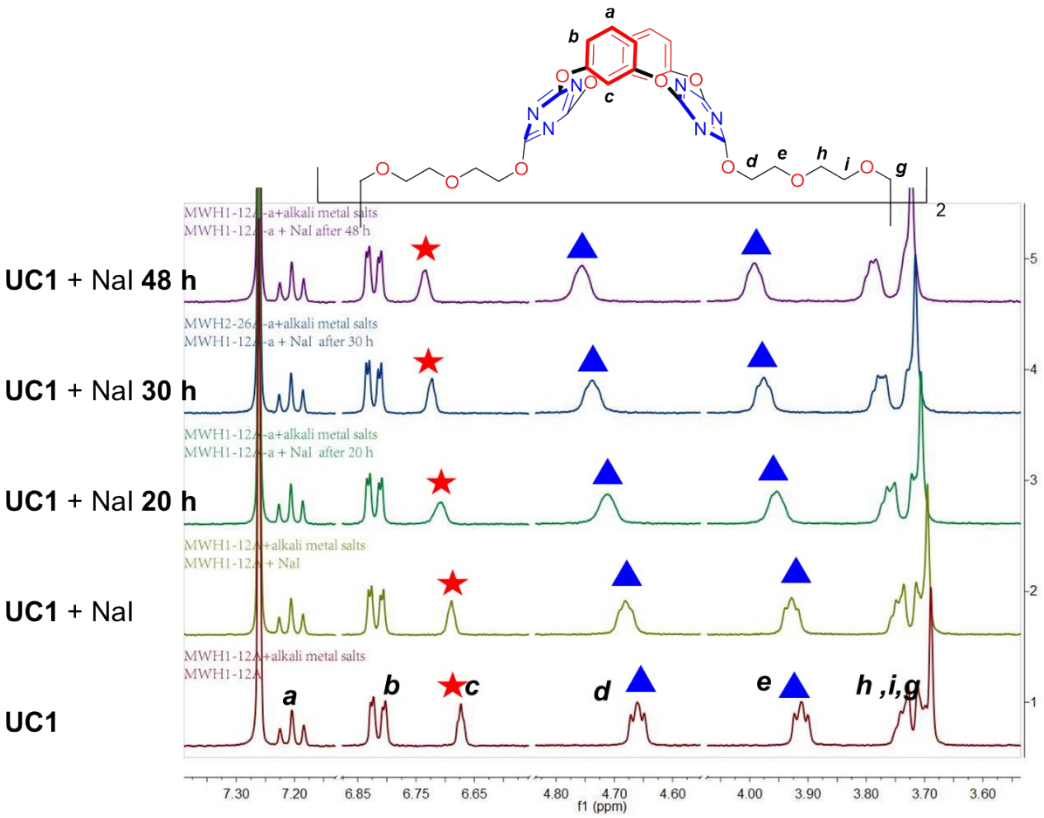

Figure S3. ^{1}H NMR spectra of solid-liquid extraction of **UC1** (10^{-3} M) and NaI at different times ("***F***")

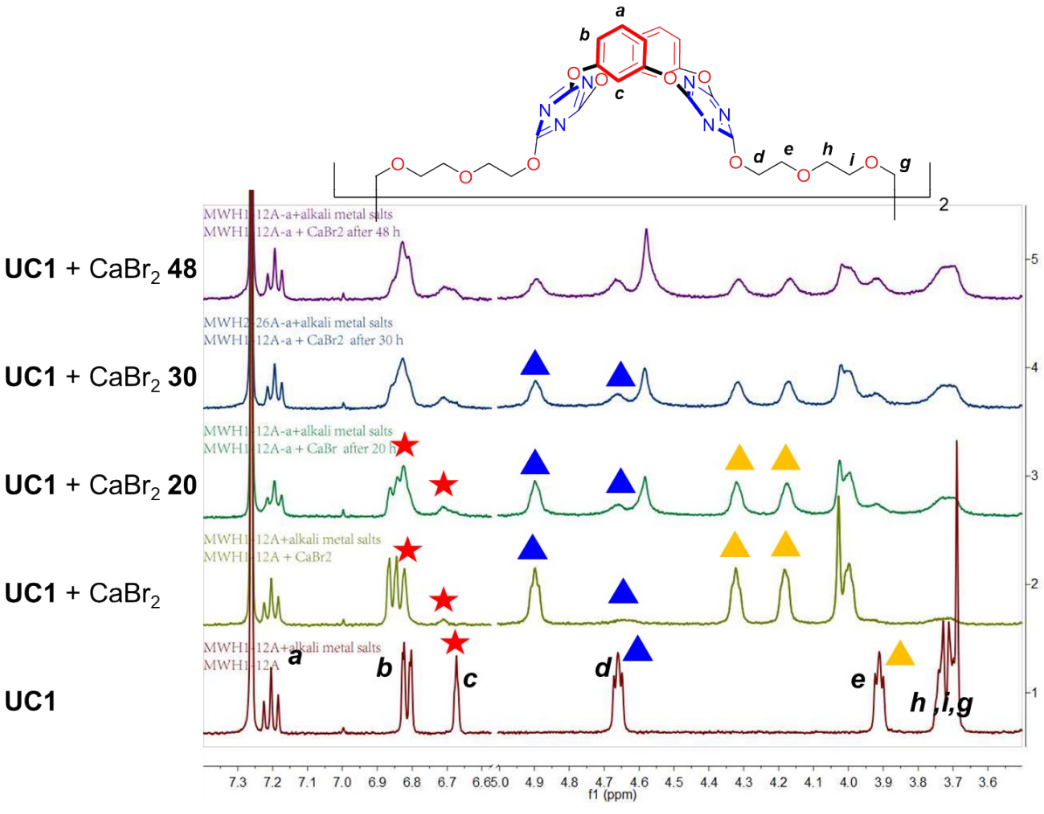

Figure S4. ^{1}H NMR spectra of solid-liquid extraction of **UC1** (10^{-3} M) and $CaBr_2$ at different times ("***S***")

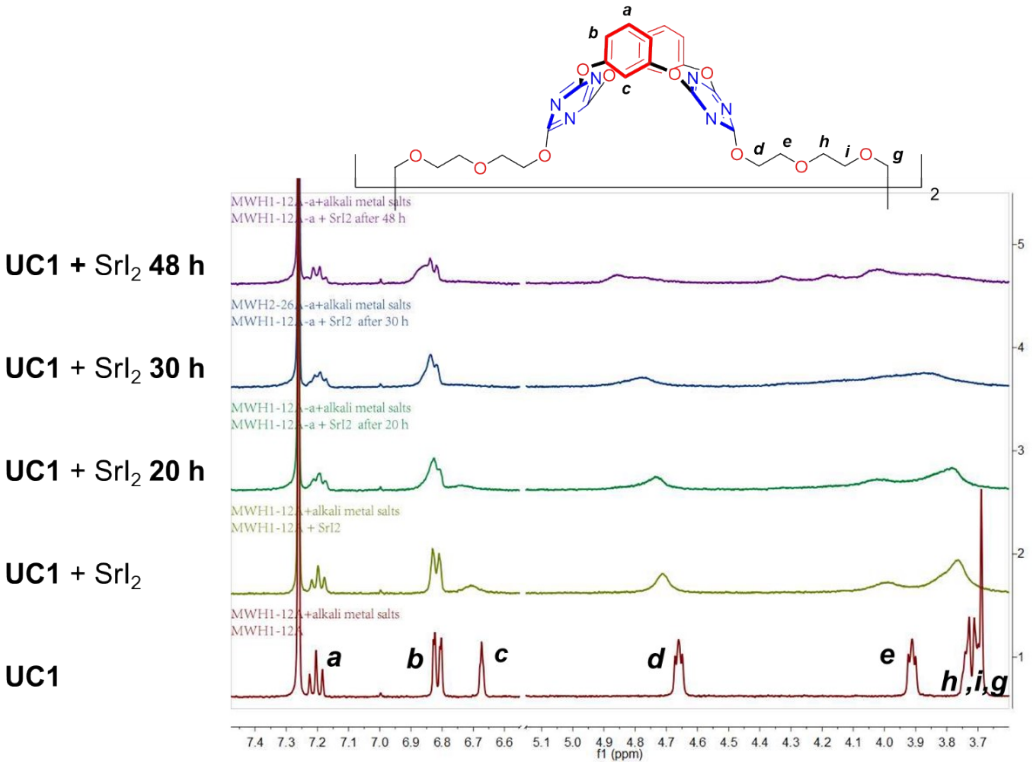

Figure S5. ^{1}H NMR spectra of solid-liquid extraction of **UC1** (10^{-3} M) and SrI_2 at different times ("***P***")

4. ^{1}H NMR Titration and Data Analysis for Ion-pair Binding.

4.1 Titration method

A host stock solution containing 1×10^{-3} M **UC1** or **UC2** in deuterated acetonitrile was prepared. 500 μL host stock solution was added to an NMR tube sealed with a rubber septum. An initial spectrum was recorded, and additional spectra were obtained after aliquots of salts (TBABr, TBAI, $NaBPh_4$, $Ca(BPh_4)_2$) solution (salt solutions were prepared by using the aforementioned host stock solution as solvent to avoid dilution) were injected sequentially using a microsyringe.

4.2 Data analysis

The cation binding was evaluated using the down-field shifts of all ethylene glycol protons and the anion association was reflected by the chemical shift changes of aromatic or hydroxyl protons. Binding constants were fitted by ***Bindfit*** using a 1:2 binding stoichiometry.

4.3 The binding between UC1 and $CaBr_2$.

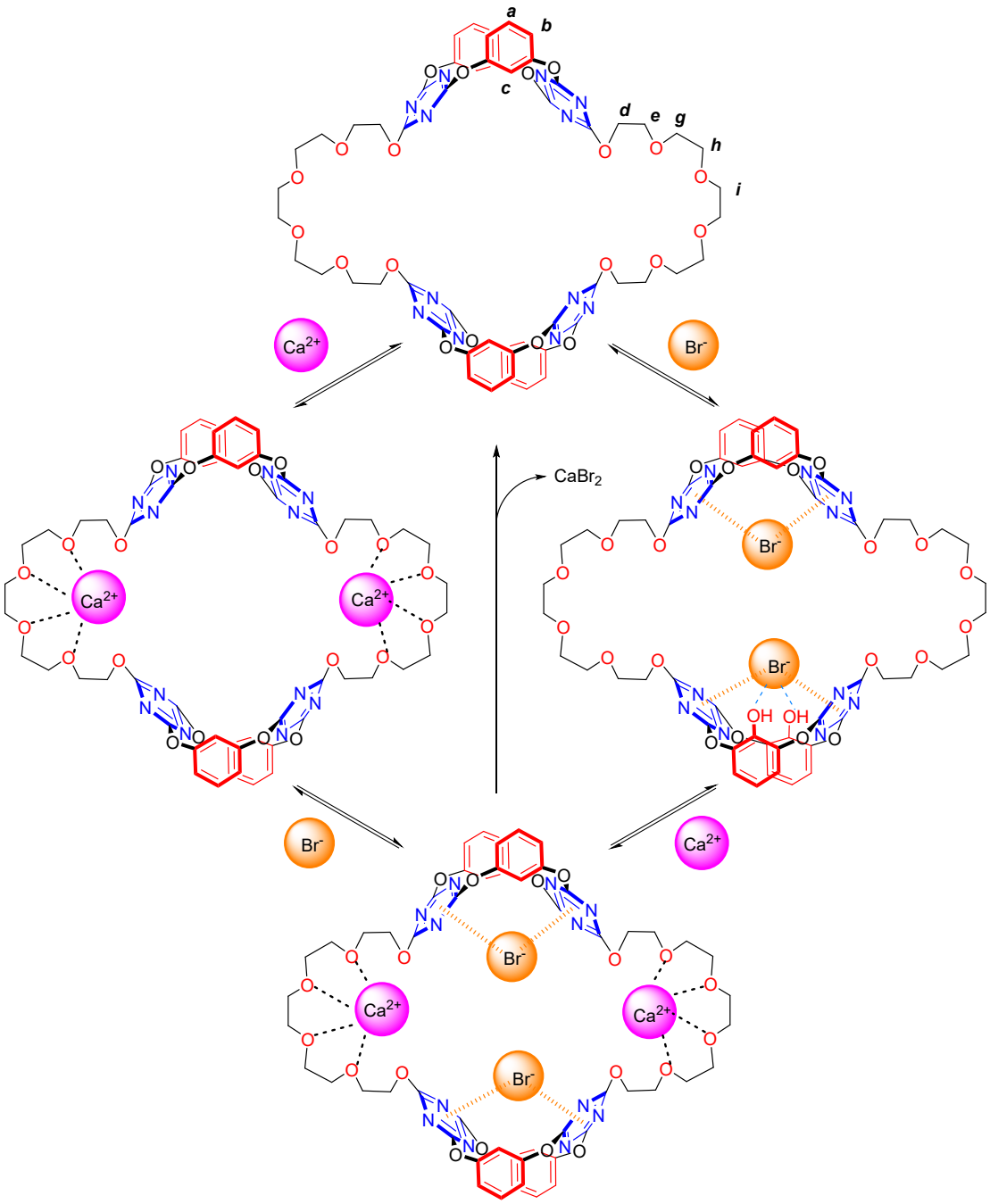

Scheme S4. The binding between **UC1** and $CaBr_2$.

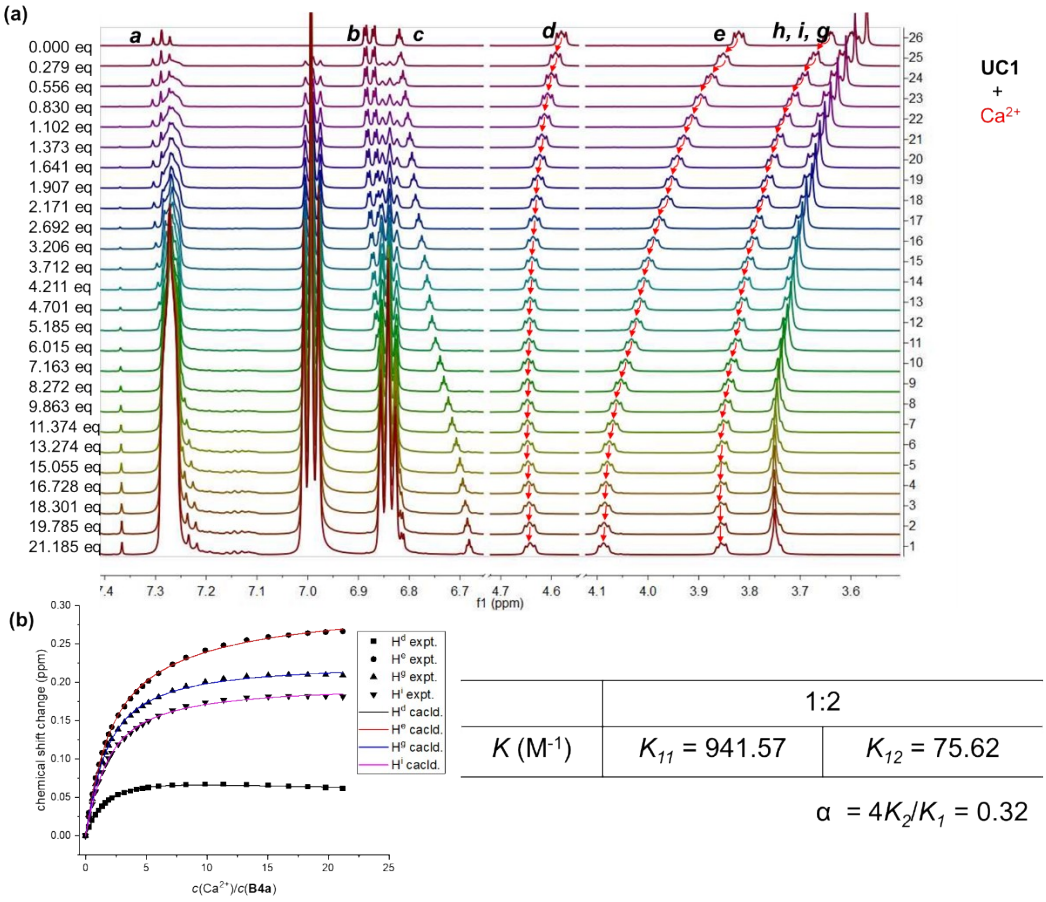

	1:2	
K (M^{-1})	K_{11} = 941.57	K_{12} = 75.62

$\alpha = 4K_2/K_1 = 0.32$

Figure S6. (a) ^{1}H NMR titration in CD_3CN of **UC1** (10^{-3} M) with increasing equivalents of Ca^{2+}, (b) Fitting the results of the titration.

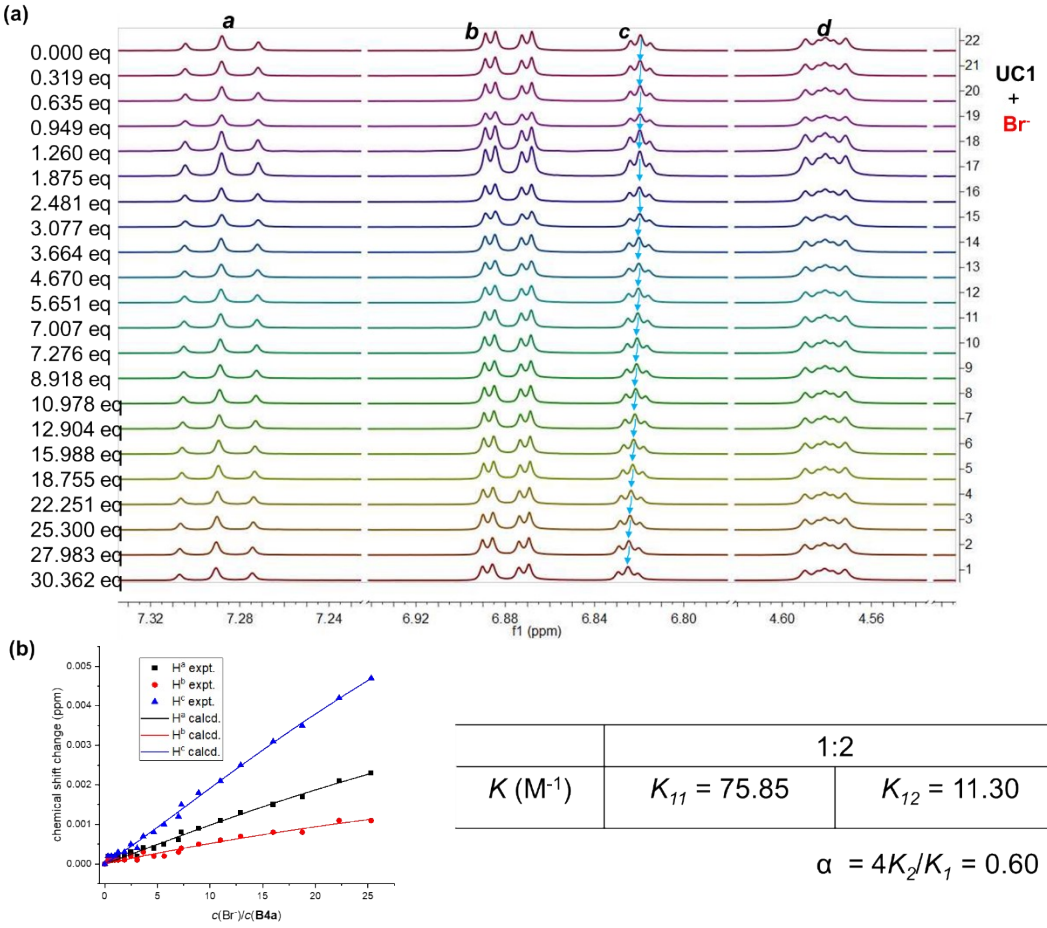

	1:2	
K (M^{-1})	K_{11} = 75.85	K_{12} = 11.30

$\alpha = 4K_2/K_1 = 0.60$

Figure S7. ^{1}H NMR titration in CD_3CN of **UC1** (10^{-3} M) with increasing equivalents of Br^-, (b) Fitting the results of the titration

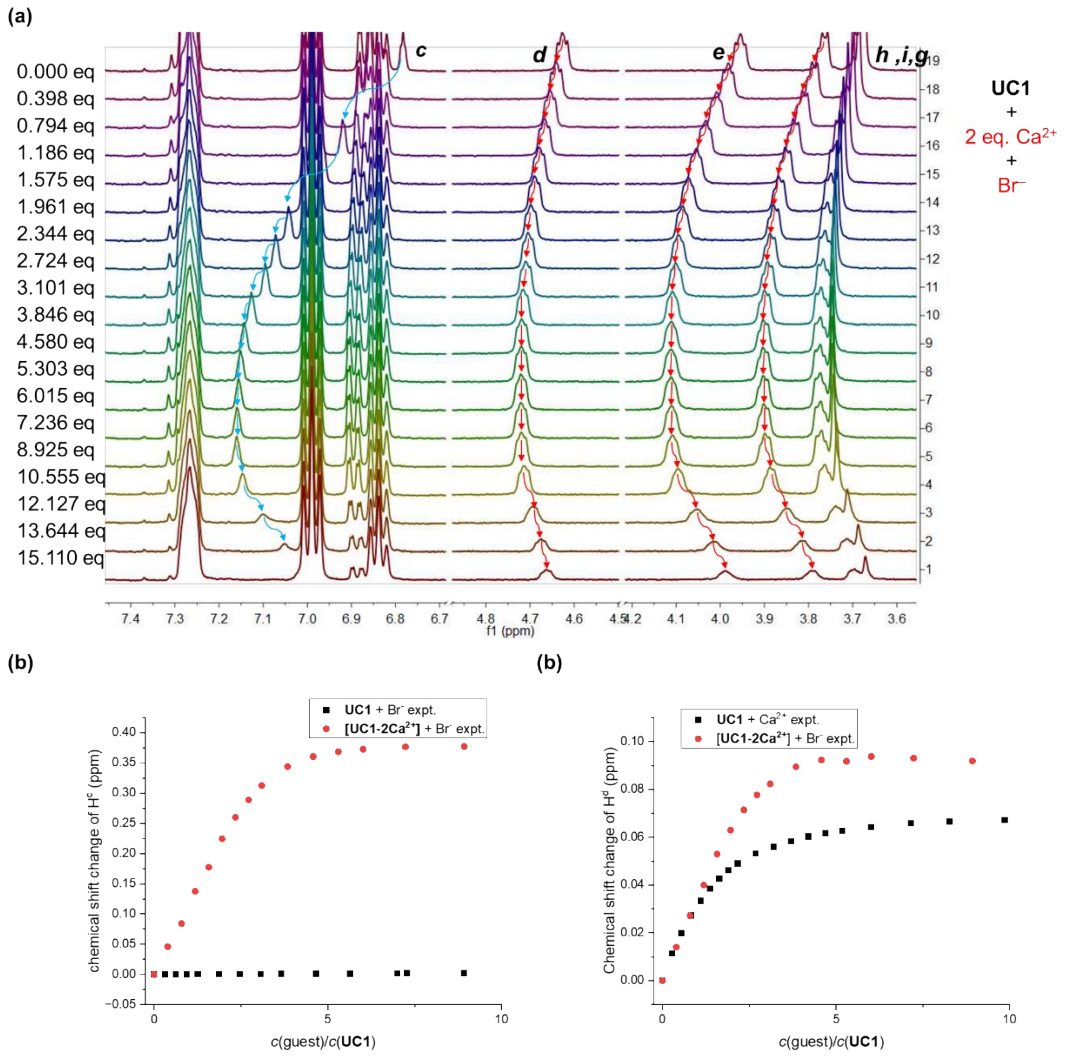

Figure S8. ^{1}H NMR titration in CD_3CN of **UC1** (1×10^{-3} M) and $Ca[B(C_6H_5)_4]_2$ (2eq) with increasing equivalents of Br^-, precipitation was observed during addition; (b) Chemical shift change of H^c (anion binding) upon titration between **UC1** and **[UC1-2Ca^{2+}]** with Br^-; (c) Chemical shift change of H^d (cation binding) upon titration between **UC1** and **[UC1-2Ca^{2+}]** with Br^-.

4.4 The binding between UC2 and NaI.

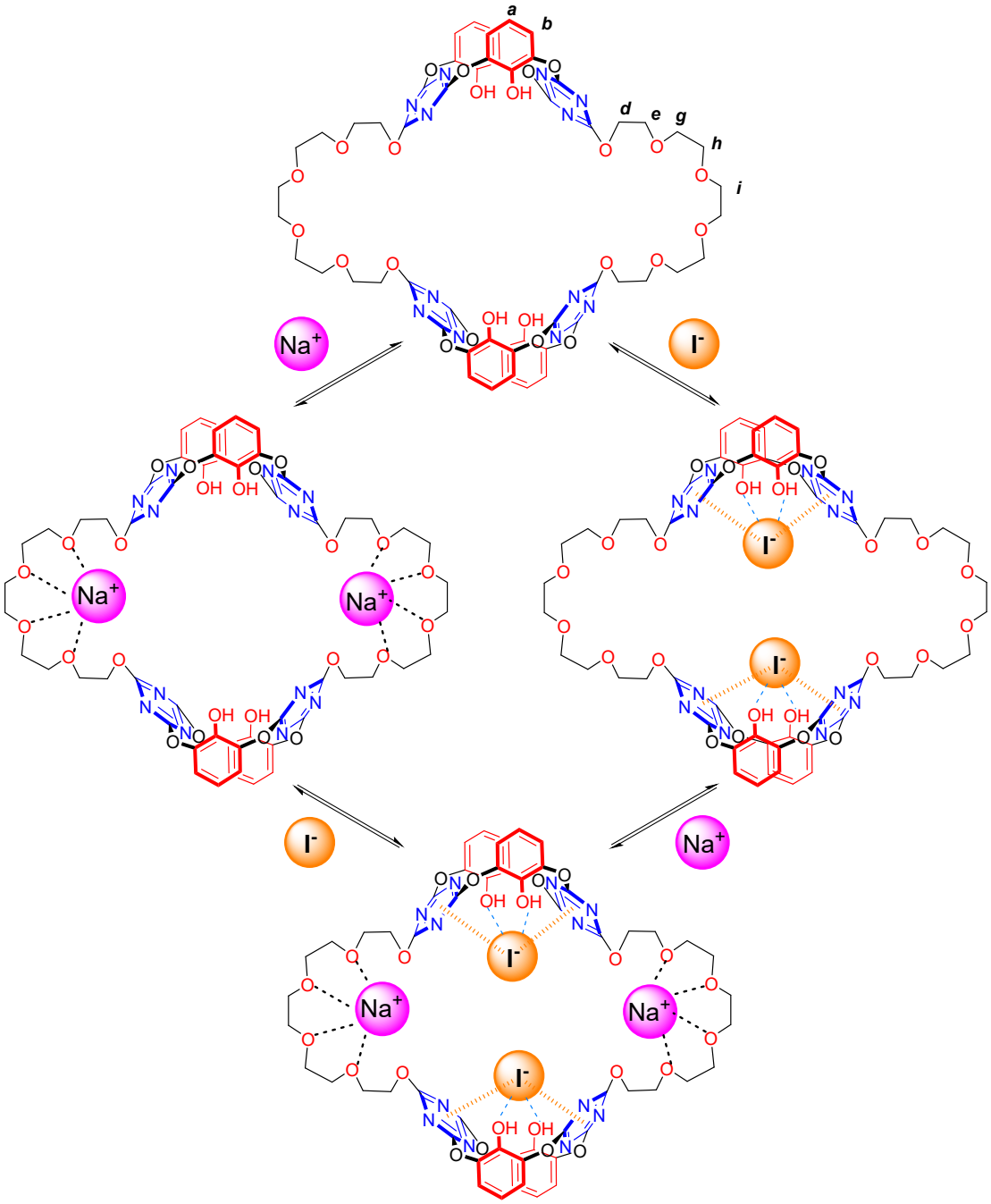

Scheme S5. The binding between **UC2** and NaI.

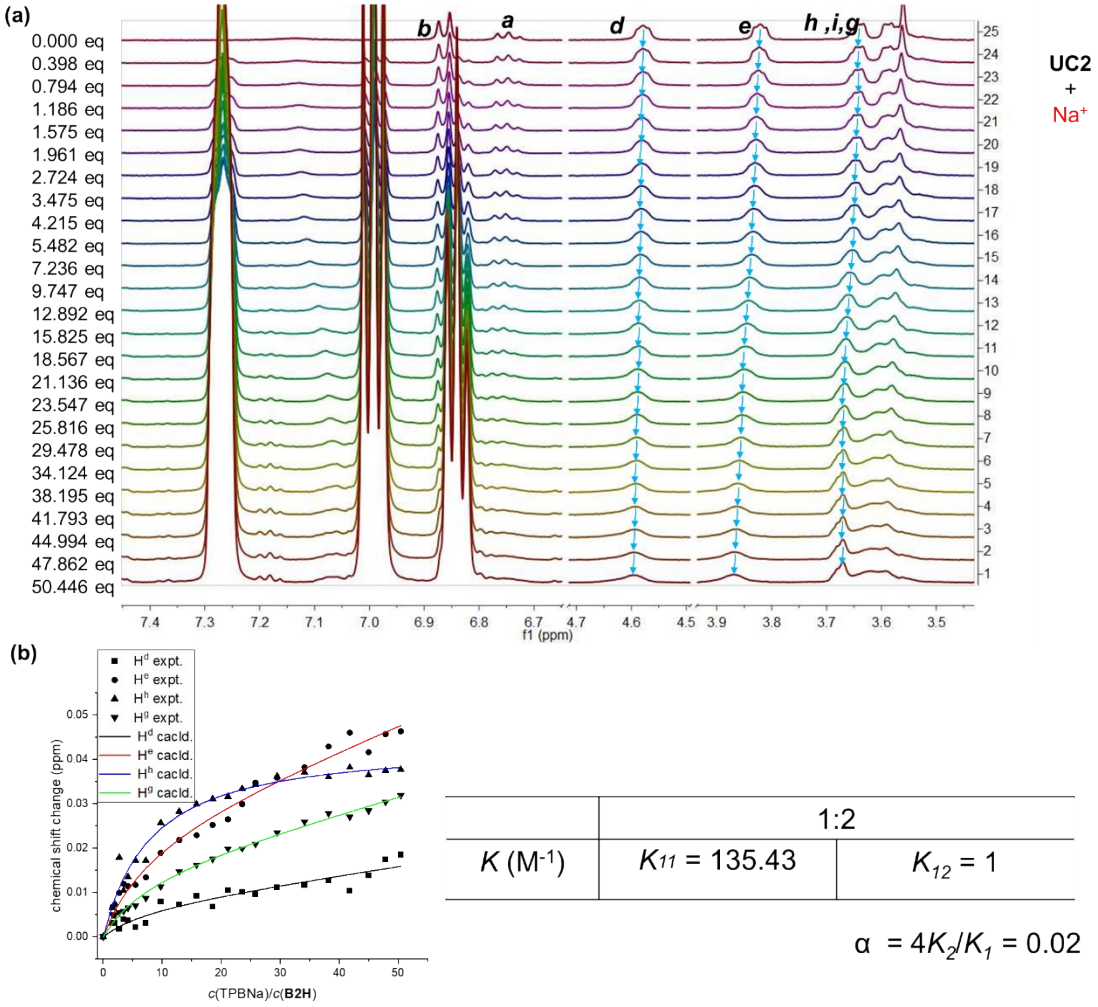

	1:2	
K (M^{-1})	K_{11} = 135.43	K_{12} = 1

$\alpha = 4K_2/K_1 = 0.02$

Figure S9. (a) ^{1}H NMR titration in CD_3CN of **UC2** (1×10^{-3} M) with increasing equivalents of Na^+, (b) Fitting results of the titration.

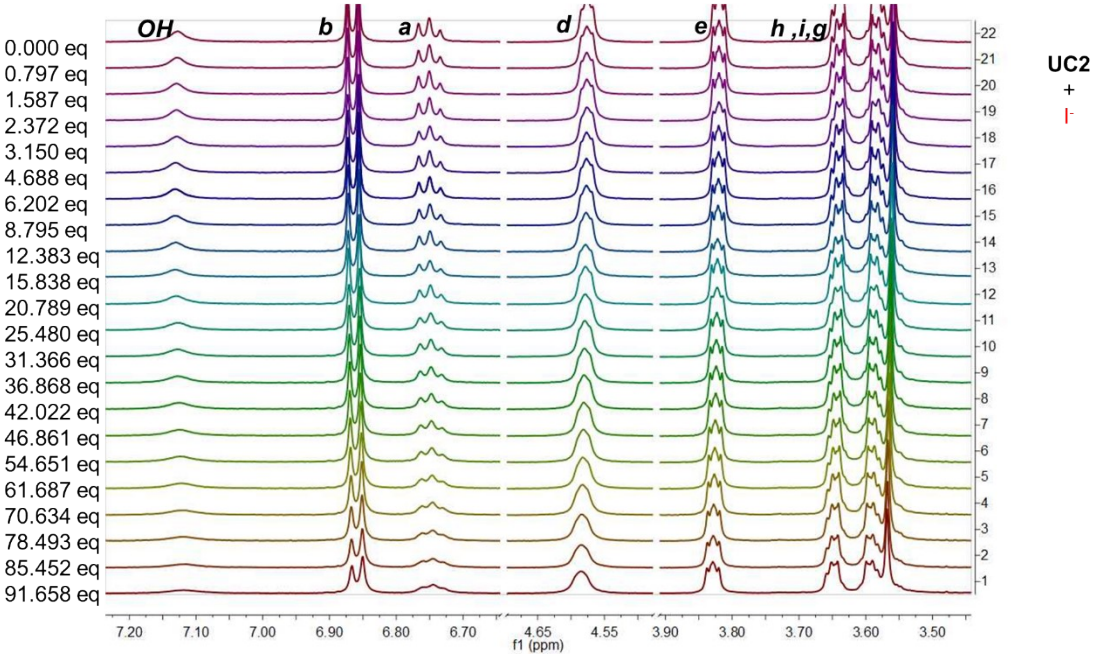

Figure S10. ^{1}H NMR titration in CD_3CN of **UC2** (1×10^{-3} M) with increasing equivalents of I^-. (The small chemical shift change makes the fitting error of the binding constant large)

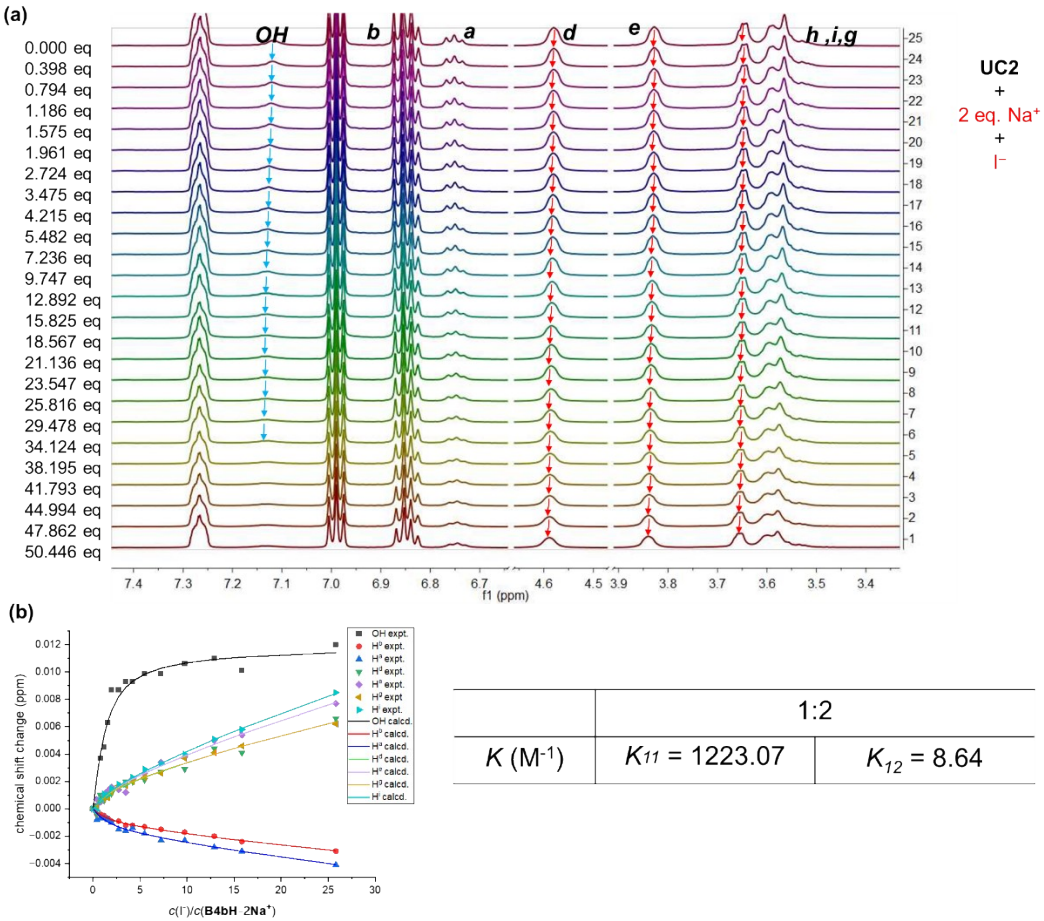

	1:2	
K (M^{-1})	K_{11} = 1223.07	K_{12} = 8.64

Figure S11. ^{1}H NMR titration in CD_3CN of **UC2** (1×10^{-3} M) and $Na[B(C_6H_5)_4]$ (2 eq.) with increasing equivalents of I^-, (b)Fitting the results of the titration.

5. X-ray Diffraction Data

Single crystal X-ray diffraction data were collected on a MM007HF Saturn724+ diffractometer using MoK/α radiation (λ= 0.71073 or 0.710747 Å) at a temperature of 173K or 298 K. The intensity data were collected by the omega scans techniques, scaled, and reduced with CrystalClear (Rigaku Inc.,2007). X-ray were provided by a fine-focus sealed X-ray tube operated at 50 KV and 24 mA.

Integrated reflection intensities were produced and the correction of the collected intensities for absorption was done using the Crystalclear (Rigaku Inc., 2007) program. The structure was solved by direct methods using SHELXT (Sheldrick, 2014) and refined using full-matrix least-squares methods in ShelXL (Sheldrick, 2014/2015). All non-hydrogen atoms were refined anisotropically, and hydrogen atoms attached to carbon atoms were fixed at their ideal positions.

Procedures for the cultivation of single crystals:

UC2-2LiClO$_4$

To obtain the complex of **UC2** and $LiClO_4$, two methods were used. One method was by slow diffusion of ether vapor into an acetonitrile/chloroform mixture (1:1, v/v) of **UC2** with a mixture of $LiClO_4$ and TBAI (1:2:2), at room temperature. The other method was by diffusion of **UC2** with a mixture of $LiClO_4$ (1:2), of acetonitrile/chloroform (1:1, v/v) in ether, at room temperature. Using these methods, a single crystal was obtained.

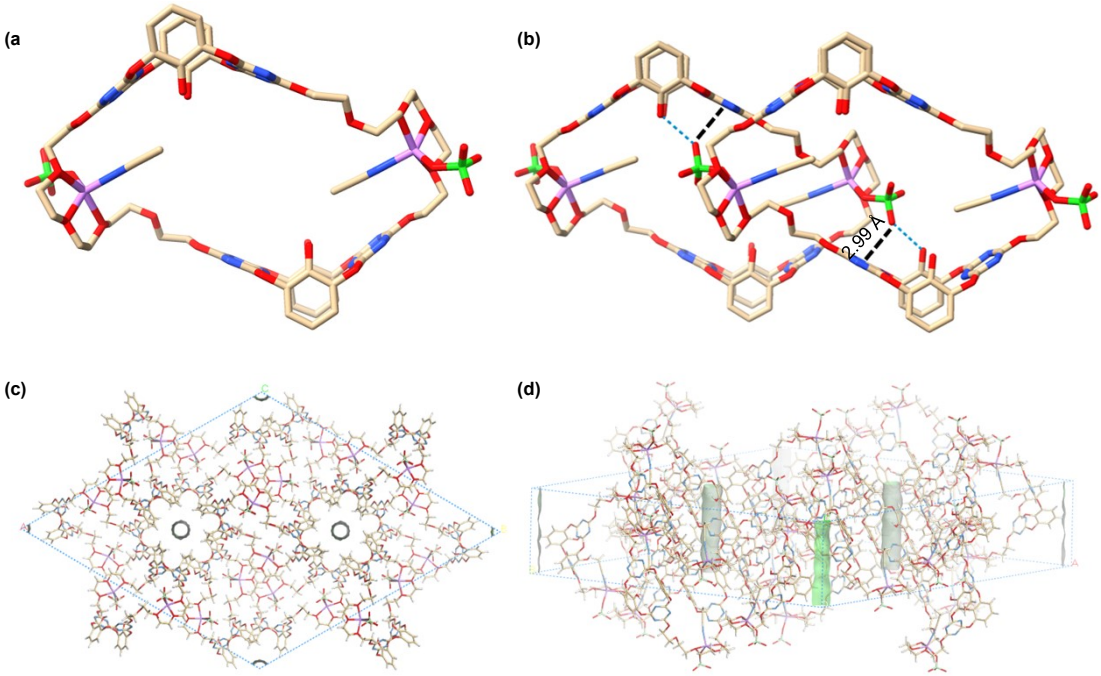

Figure S12. (a), (b) The crystal structure of [**UC2-2LiClO$_4$**], (c) Channel projected from [001] direction of [**UC2-2LiClO$_4$**] crystal, (d) Channel seen from an arbitrary direction of [**UC2-2LiClO$_4$**] crystal.

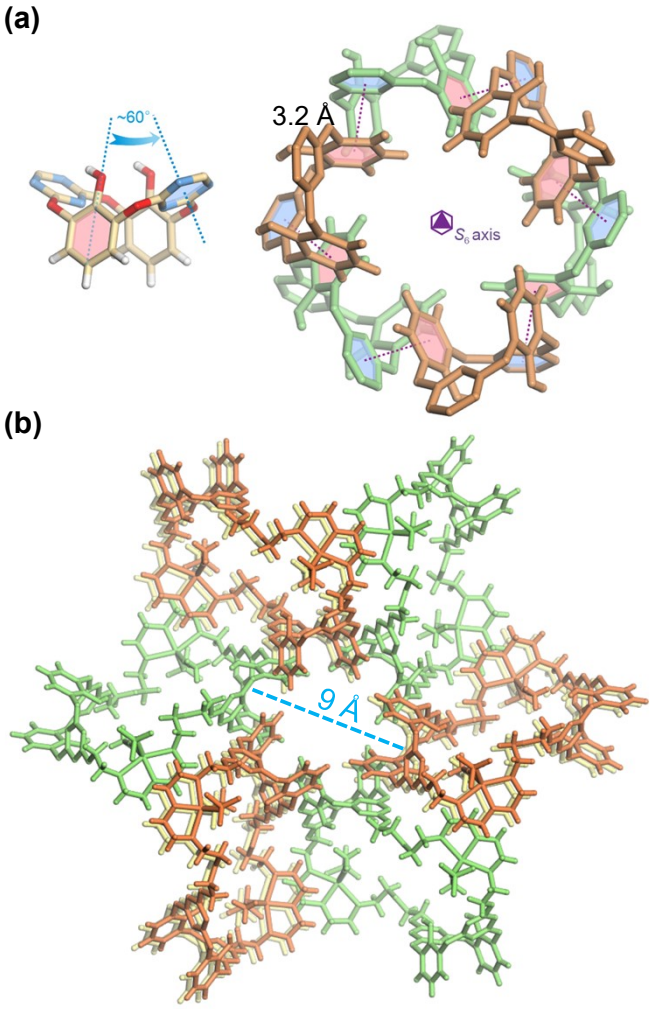

Figure S13. (a) The local stacking mode of oxacalix[2]arene[2]trizaine subunits participating in a single hexagonal plum blossom-shaped channel, (b) The arrangement of the complex contributing to a single hexagonal plum blossom-shaped channel.

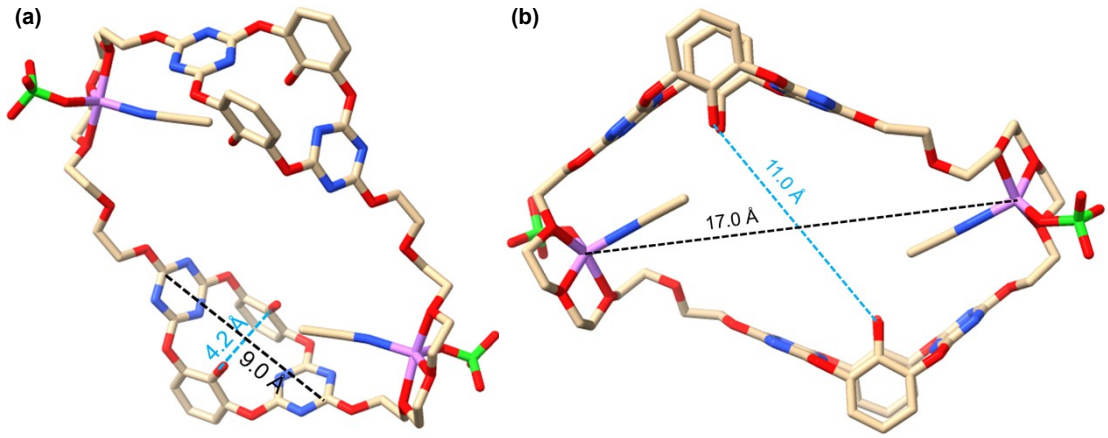

Figure S14. (a) The intrinsic cavity of IPOF (a) the smallest, (b) the middle.

Table S2. Crystal data and structure refinement for **[UC2-2LiClO$_4$]**

Identification code	**[UC2-2LiClO$_4$]**
CCDC	2417978
Empirical formula	C34 H37 Cl Li N9 O16
Formula weight	870.11
Temperature	172.99(10) K
Wavelength	1.54184 Å
Crystal system	Trigonal
Space group	*R*−3
Unit cell dimensions	*a* = 42.5681(8) Å, α = 90°.
	b = 42.5681(8) Å, β = 90°
	c = 11.8355(2) Å, γ = 120°
Volume	18573.1(8) Å^3
Z	18
Density (calculated)	1.400 Mg/m^3
Absorption coefficient	1.526 mm^{-1}
F(000)	8136
Crystal size	0.4 × 0.025 × 0.02 mm^3
Theta range for data collection	2.076 to 76.666°.
Index ranges	-45<=h<=52, -43<=k<=51, -14<=l<=8
Reflections collected	21211
Independent reflections	8181 [R_{int} = 0.0591]
Completeness to theta = 67.684°	97.60%
Absorption correction	Semi-empirical from equivalents
Max. and min. transmission	1.00000 and 0.47215
Refinement method	Full-matrix least-squares on F2
Data / restraints / parameters	8181 / 1 / 555
Goodness-of-fit on F2	1.048
Final R indices [I>2sigma(I)]	R_1 = 0.0693, wR_2 = 0.2009
R indices (all data)	R_1 = 0.0929, wR_2 = 0.2203
Extinction coefficient	n/a
Largest diff. peak and hole	1.562 and −0.498 e·Å^{-3}

UC1-2CaBr$_2$

The crystal structure of the 1:2 complex of **UC1** with $CaBr_2$ was obtained by slow diffusion of ether vapor into a mixed solution of acetonitrile and chloroform (9:1, v/v) containing the mixture of **UC1** and $CaBr_2$ (1:2), at room temperature.

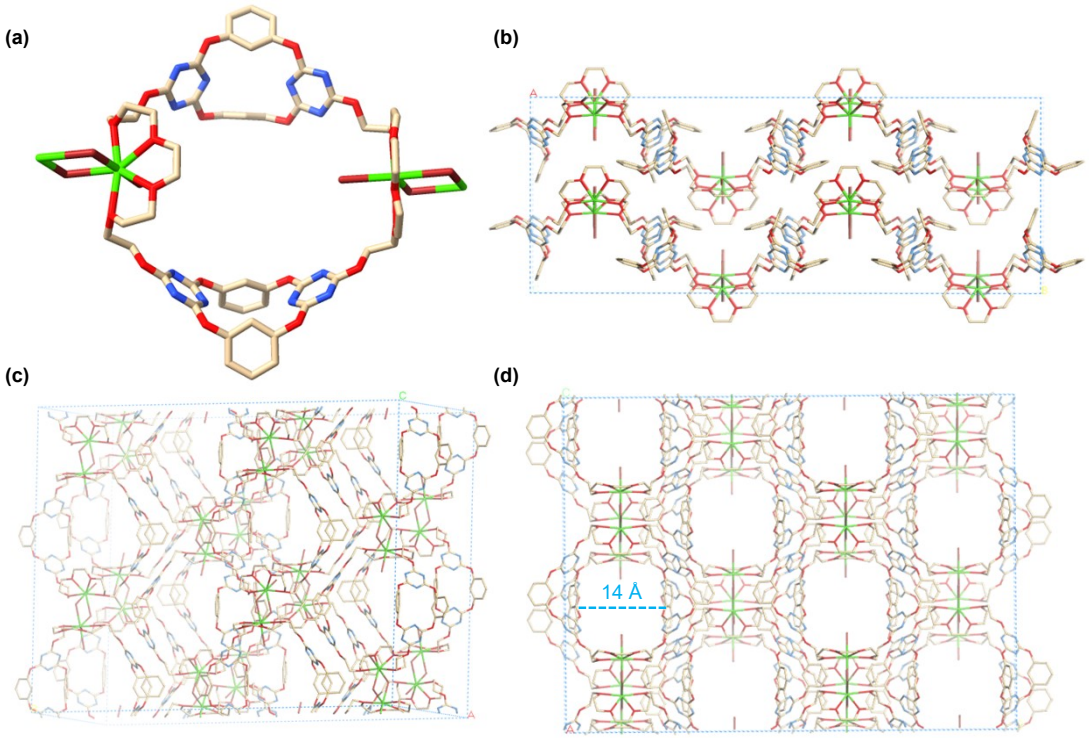

Figure S15. (a) The crystal structure of [**UC1-2CaBr$_2$**], (b) Crystal structure projected from [001] direction, (c) Illustration of stacking mode of complex along [010] direction, showing a short contact among triazine rings, (d) Crystal structure and channel projected from [100] direction (the unit cell is 4-times extended for clarity).

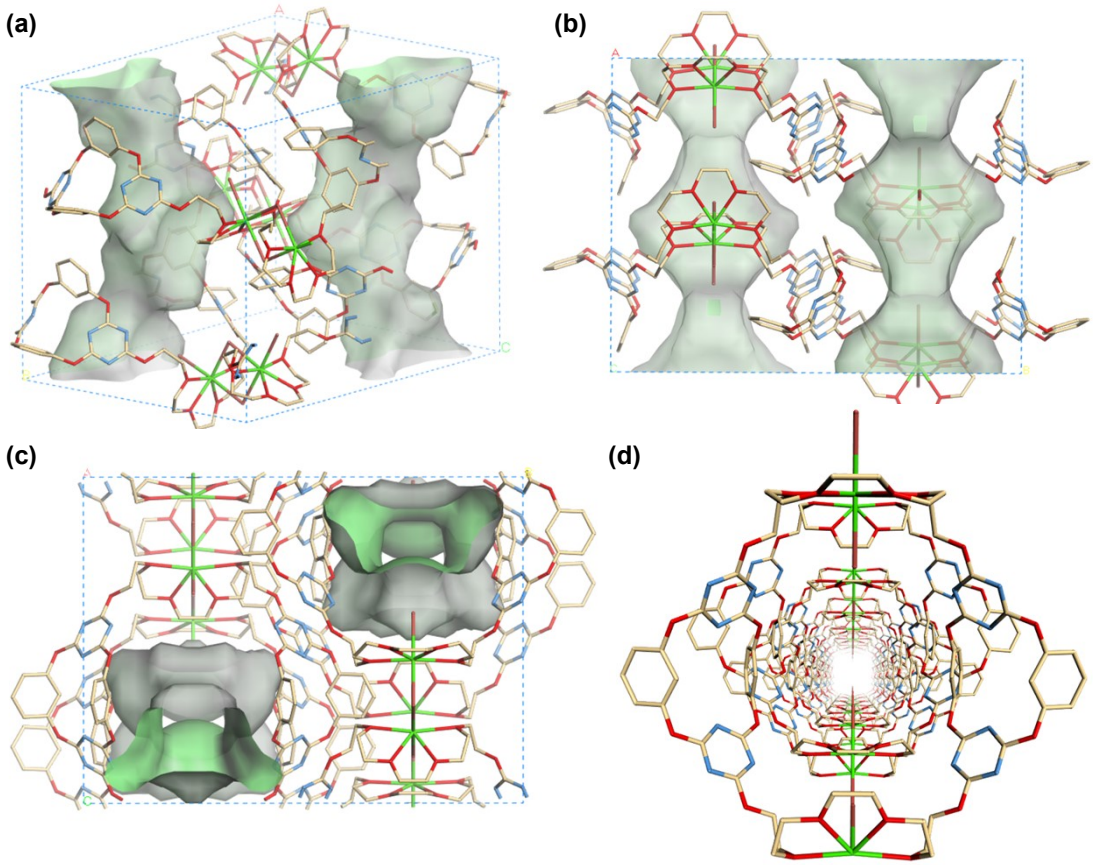

Figure S16. (a) channel seen from an arbitrary direction of [**UC1-2CaBr$_2$**], (b) channel projected from [001] direction of [**UC1-2CaBr$_2$**]; (c) Channel projected from [100] direction of [**UC1-2CaBr$_2$**], (d) Perspective view of the channel formed by packing of the complex cavity.

Table S3. Crystal data and structure refinement for [**UC1-2CaBr$_2$**]

Identification code	[**UC1-2CaBr$_2$**]	
CCDC	2417979	
Empirical formula	C56 H56 Br4 Ca2 N12 O20	
Formula weight	1616.92	
Temperature	173.15 K	
Wavelength	0.71073 Å	
Crystal system	Orthorhombic	
Space group	*Pnma*	
Unit cell dimensions	a = 19.0358(6) Å	a = 90°.
	b = 24.8790(7) Å	b = 90°.
	c = 18.4923(9) Å	g = 90°.
Volume	8757.8(6) Å^3	
Z	4	
Density (calculated)	1.226 Mg/m^3	
Absorption coefficient	2.016 mm^{-1}	
F(000)	3264	
Crystal size	0.182 x 0.112 x 0.061 mm^3	
Theta range for data collection	1.535 to 27.499°.	
Index ranges	-24<=h<=24, -29<=k<=32, -23<=l<=23	
Reflections collected	57836	
Independent reflections	10247 [R(int) = 0.0861]	
Completeness to theta = 25.242°	99.7 %	
Absorption correction	Semi-empirical from equivalents	
Max. and min. transmission	1.00000 and 0.42876	
Refinement method	Full-matrix least-squares on F^2	
Data / restraints / parameters	10247 / 88 / 453	
Goodness-of-fit on F^2	1.043	
Final R indices [I>2sigma(I)]	R1 = 0.0931, wR2 = 0.2590	
R indices (all data)	R1 = 0.1582, wR2 = 0.2974	
Extinction coefficient	n/a	
Largest diff. peak and hole	2.636 and -0.769 e.Å^{-3}	

6. Iodine Vapor Capture

Time-dependent iodine vapor uptake experiments based on gravimetric measurements were performed in the following procedure: 3 mg of each IPOF was weighed and placed in pre-weighed glass vessels (2 mL), respectively. Thereupon, the vessels were loaded in bigger sealed vials (20 mL) containing 500 mg of iodine, followed by the recording of their changing mass over time. The iodine uptake capacities for IPOF were calculated by weighted gains: C (mg/mg) = $(W_a - W_b)/W_b$, where C is the iodine uptake capacity and W_a and W_b are the mass weight of IPOF before and after iodine vapor adsorption.

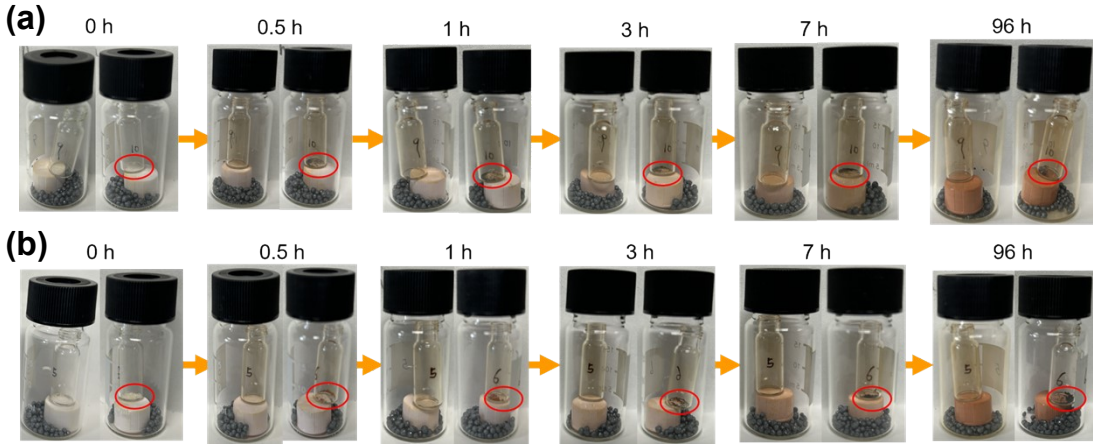

Figure S17. The picture showed the color changes of IPOF (a) **[UC2-2LiClO$_4$]**, (b) **[UC1-2CaBr$_2$]**.

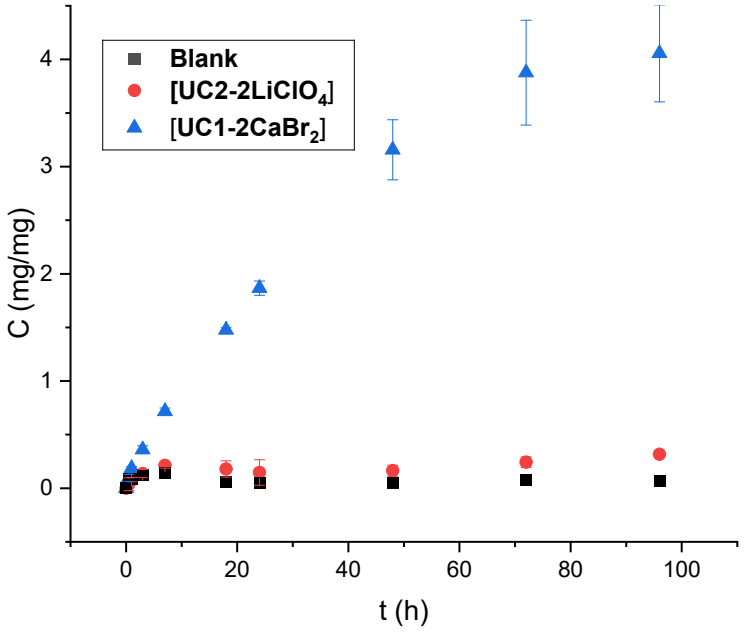

Figure S18. Time-dependent iodine vapor uptake at room temperature of IPOF.

The kinetics data of iodine vapor adsorption were fitted by pseudo-second order (PSO) model expressed as equation[4]:

$$\frac{dq_t}{dt} = k_2 (q_e - q_t)^2$$

$$q_t = \frac{q_e^2 k_2 t}{1 + q_e k_2 t} \qquad (1)$$

Where k_2 (mg mg^{-1} h^{-1}) stands for the corresponding rate constant, q_e and q_t are the adsorption capacity at equilibrium and time t (h), respectively.

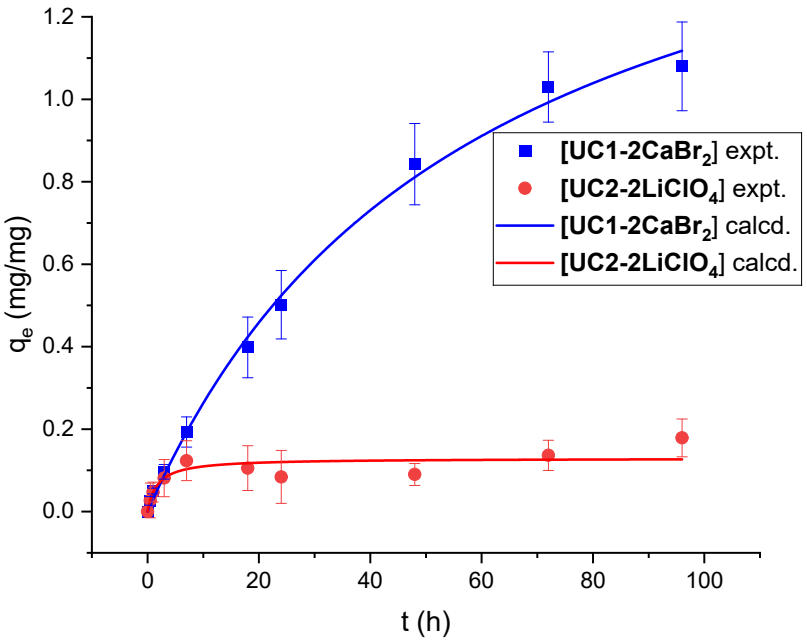

Figure S19. Fitting results of adsorption of IPOF.

7. Theoretical Calculations

To evaluate the adsorption performance of the porous crystalline material for molecular iodine, adsorption isotherm simulations were conducted using the Metropolis Monte Carlo (MMC) method. The calculations were performed at a constant temperature of 298.0 K, using the Dreiding force field, incorporating modified Ewald summation for electrostatic potential and standard van der Waals interactions. For each fugacity point on the isotherm, the simulation consisted of 200,000 equilibration steps followed by 2,000,000 production steps. The simulation results spanned 10 fugacity points ranging from 0.5 Pa to 5.0 Pa and 25 fugacity points ranging from 5.0 Pa to 40.0 Pa (the saturated vapor pressure of solid I_2 at 298 K, see Table S4).

Density functional theory (DFT) calculations for the binding energy were performed using the Gaussian 16 software package. Considering that iodine adsorption is primarily driven by intermolecular non-covalent interactions, we employed the ωB97X-D functional, which offers accurate dispersion and long-range corrections, in conjunction with the def2-TZVP basis set which includes intrinsic pseudopotentials, for both light atoms and iodine.

Table S4. Simulated absorption isotherms of iodine with IPOFs **[UC1-2CaBr$_2$]** and **[UC2-2LiClO$_4$]**

Fugacity (kPa)	Loadings (mg/mg)	
	[UC1-2CaBr$_2$]	**[UC2-2LiClO$_4$]**
0.0000	0.0000	0.0000
0.0005	0.2935	0.0400
0.0010	0.6308	0.0641
0.0015	0.9762	0.0775
0.0020	1.1218	0.0857
0.0025	1.1547	0.0869
0.0030	1.3466	0.0935
0.0035	1.3686	0.1013
0.0040	1.2887	0.1062
0.0045	1.3005	0.0985
0.0050	1.3479	0.1176
0.0064	1.4336	0.1216
0.0078	1.4770	0.1295
0.0092	1.4893	0.1262

0.0106	1.4940	0.1308
0.0120	1.5210	0.1340
0.0134	1.6620	0.1354
0.0148	1.7022	0.1412
0.0162	1.6453	0.1362
0.0176	1.6069	0.1438
0.0190	1.6414	0.1437
0.0204	1.5705	0.1428
0.0218	1.6096	0.1436
0.0232	1.6306	0.1440
0.0246	1.6243	0.1479
0.0260	1.6114	0.1454
0.0274	1.6354	0.1457
0.0288	1.6374	0.1488
0.0302	1.6336	0.1484
0.0316	1.6076	0.1495
0.0330	1.6627	0.1477
0.0344	1.6784	0.1521
0.0358	1.6677	0.1511
0.0372	1.6991	0.1588
0.0386	1.6913	0.1524
0.0400	1.6945	0.1499

8. Copies of ^{1}H and ^{13}C NMR Spectra

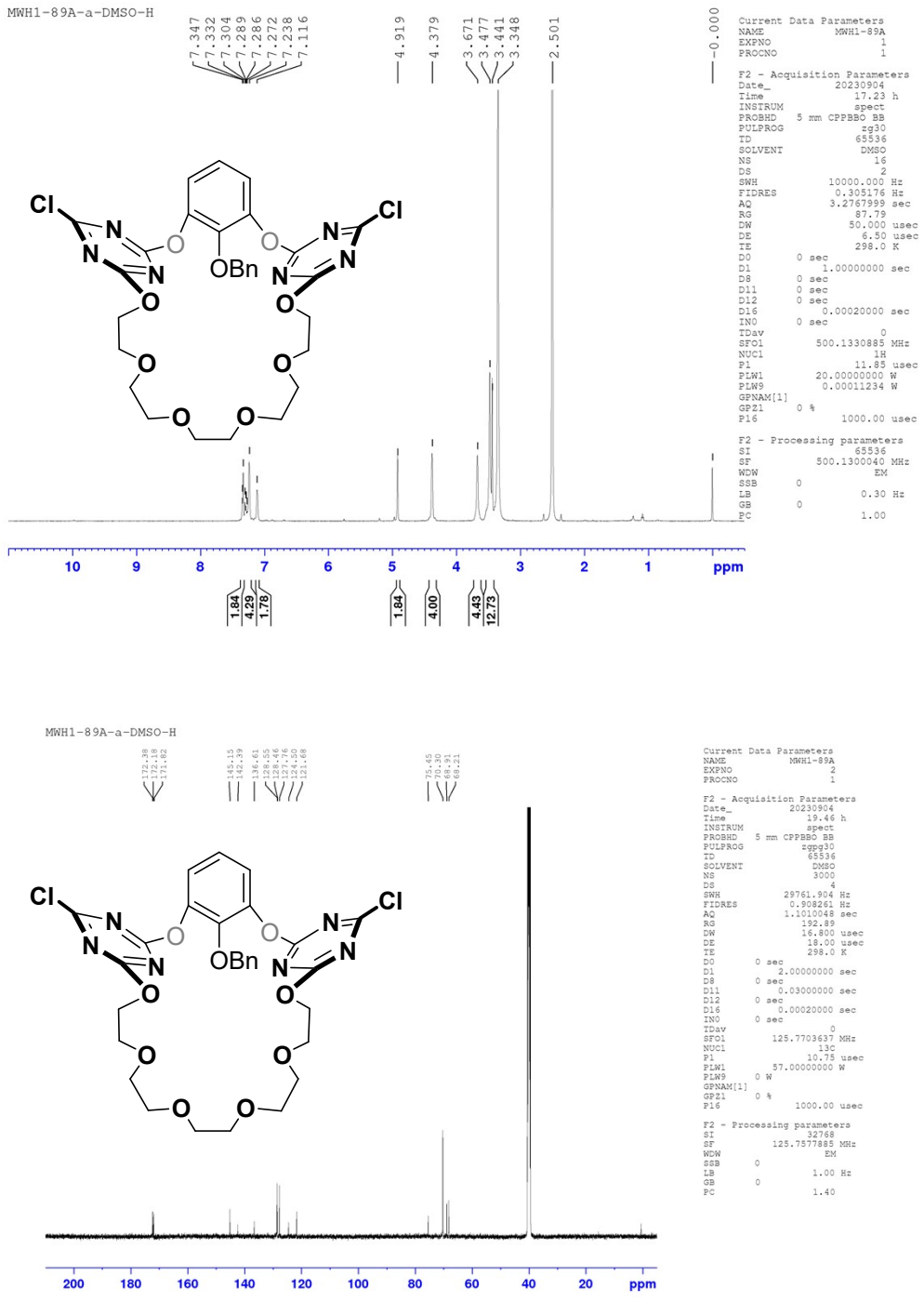

^{1}H and ^{13}C NMR of **1b** in DMSO-d_6

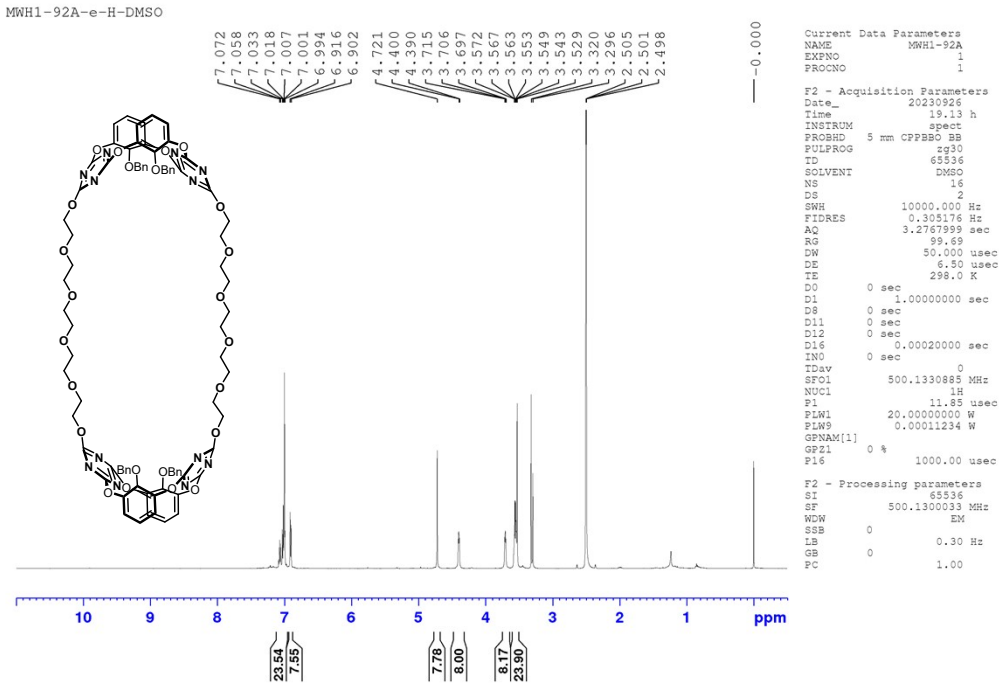

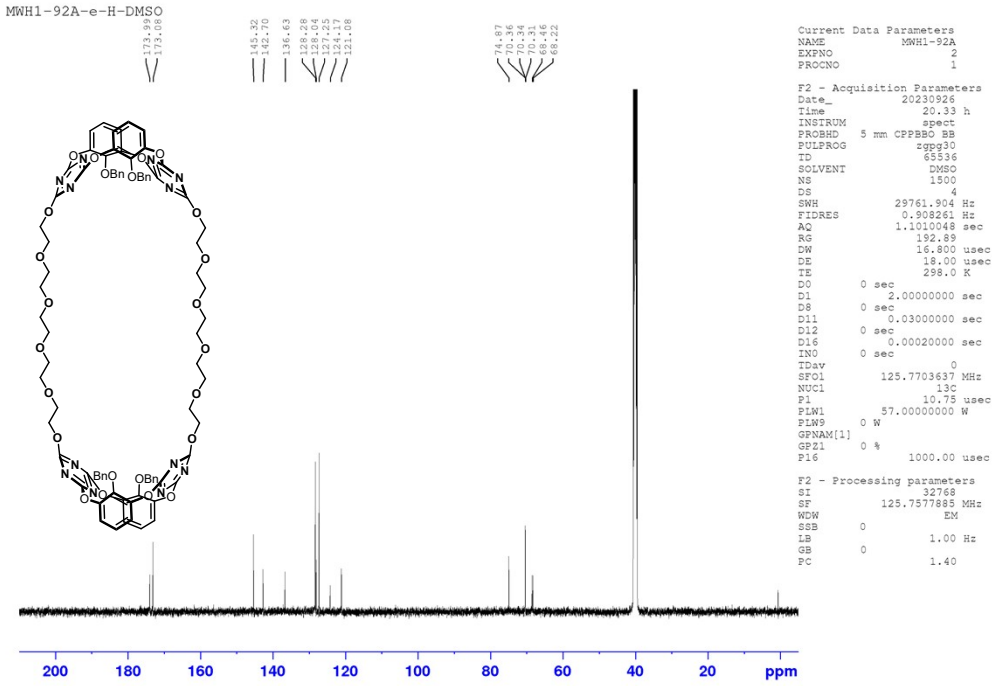

^{1}H and ^{13}C NMR of **4** in DMSO-d_6

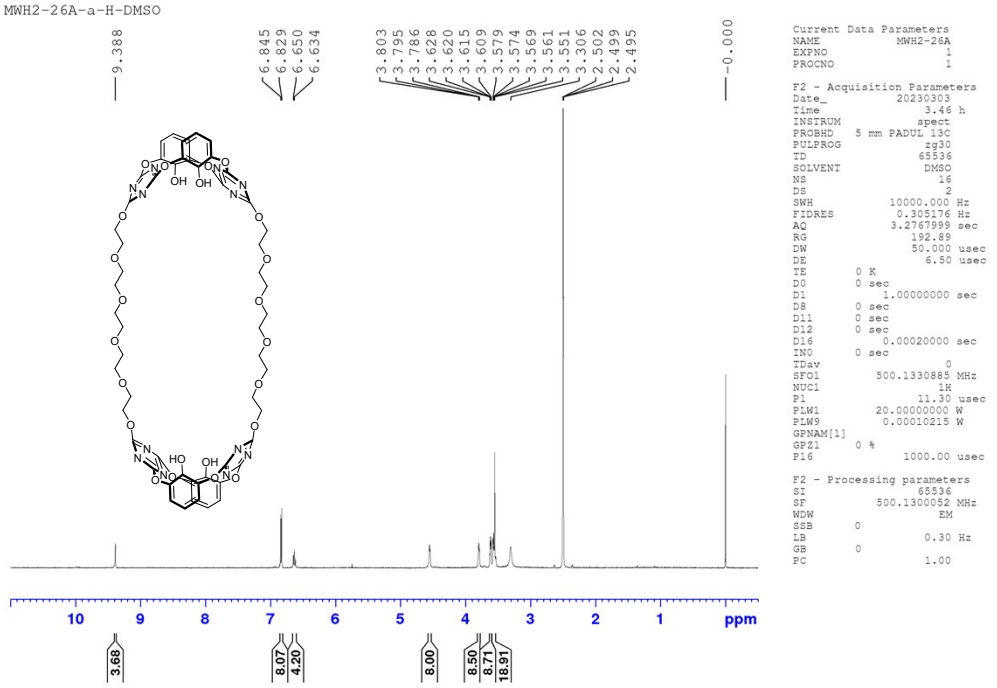

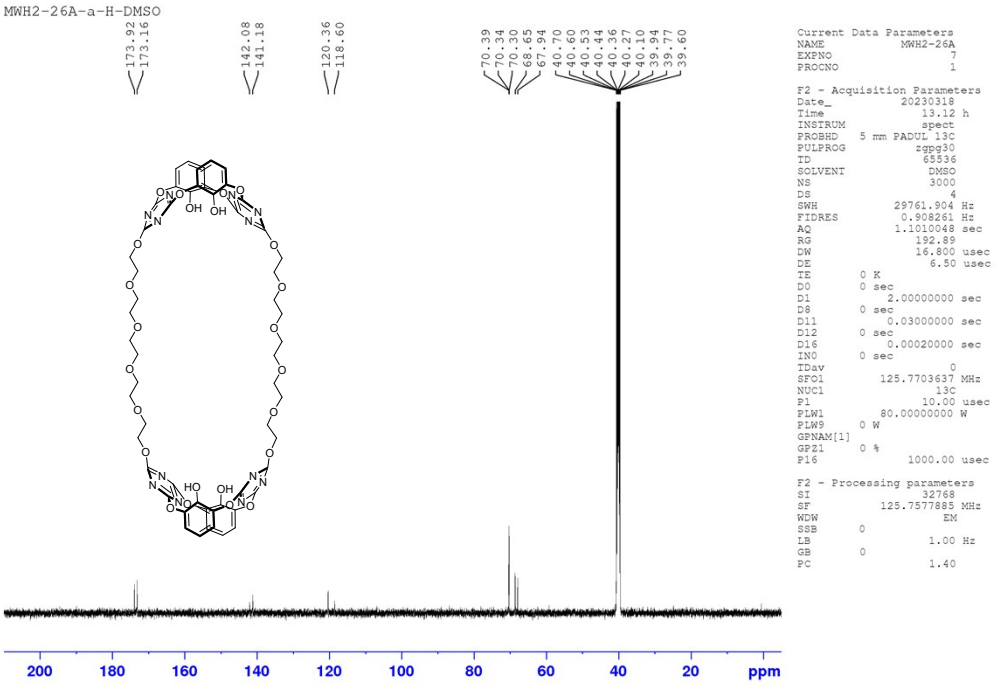

^{1}H and ^{13}C NMR of **UC2** in DMSO-d_6

9. References

[1] Luo, J., Ao, Y.-F., Wang, Q.-Q. and Wang, D.-X. *Angew. Chem. Int. Ed*., 2018, **57**, 15827–15831.

[2] Luo, J.; Ao, Y.-F.; Malm, C.; Hunger, J.; Wang, Q.-Q. and Wang, D.-X. *Dalton Trans*., 2018, **47**, 7883–7887.

[3] Michihata, N.; Kaneko, Y.; Kasai, Y.; Tanigawa, K.; Hirokane, T.; Higasa, S. and Yamada, H., *J. Org. Chem*., 2013, **78**, 4319–4328.

[4] Wang, J. L. and Guo, X. *J. Hazard. Mater*., 2020, **390**, 122156–122174.